

The influence of pH on properties of nanocrystalline ZnSe thin films

DEEP SHIKHA^{a,b,*}, V. MEHTA^b, J. K. SHARMA^a, JEEWAN SHARMA^c

^aDepartment of Physics, Maharishi Markandeshwar University, Mullana, Ambala-133207 India

^bPG Department of Physics, Sri Guru Teg Bahadur Khalsa College, Anandpur Sahib-140118 India

^cDepartment of Nanotechnology, Sri Guru Granth Sahib University, Fatehgarh Sahib – 140407 India

The structural, optical and electrical properties of ZnSe films deposited by chemical bath deposition method were investigated as a function of pH(11.0 to13.0). XRD studies showed that films deposited were polycrystalline in nature with zinc-blende structure and a strong [111] texture. The grain size increases as pH increases. From the optical studies the band gap is obtained and showed that it varies inversely with pH and in electrical studies it was observed that both dark and photoconductivity increases as the particle size increases.

(Received January 5, 2015; accepted April 5, 2016)

Keywords: ZnSe, Chemical bath deposition, Structural, Optical and electrical

1. Introduction

ZnSe nanoparticles have wide-ranging applications because it has wide and direct band gap. Bulk ZnSe has a band gap of 2.58 eV [1-2] which in nanocrystals can varied up to 3.5 eV. It is transparent over a wide range of visible spectrum and has a relatively large non-linear optical coefficient. It is well known as a high refractive index material in multilayer film combinations and as an infrared antireflection coating of solar cells, due to its wide band gap. ZnSe possesses unique optical and photovoltaic properties and exhibits great potential applications, such as blue–green light emitting diodes, photoluminescent and electroluminescent devices, lasers, thin film solar cell non-linear optical crystal and infrared optical materials [3-4]. It is also used to increase the open circuit voltage of solar cells [5]. The properties of nanocrystals prepared by different methods are critically dependent on the nature of preparation techniques. Several methods have been used to make nanocrystalline thin films of ZnSe such as physical vapor deposition [6], pulsed laser deposition [7], molecular beam epitaxy [8], electro-chemical methods [9], spray pyrolysis [10], sol–gel deposition [11], chemical vapor deposition [12], chemical depositions [13] etc. Chemical bath deposition (CBD) is an excellent method to prepare nanocrystalline thin films because crystals in most as-deposited films are very small but the nanocrystalline films and nanocrystals (NCs) are formed by controlling the rate of these reactions, so that they occur slowly enough to allow the (NCs) either to form gradually on the substrate or to diffuse there and adhere either to substrate itself (at the early stages of deposition) or to the growing film, rather than aggregate into larger particles in solution and precipitate out [13].

For the deposition of ZnSe NCs the rate control can be maintained by generating selenide ions slowly in the deposition solution. The rate generation of selenide ions and hence the particle size is controlled through a number of parameters such as pH, substrate temperature, concentration of reacting species and deposition time etc. In this paper, we have reported the preparation of nanocrystalline ZnSe thin films in the alkaline medium at different pH of Zn²⁺ ion. The structural properties have been monitored by X-ray diffraction (XRD) while the optical characterization has been done through UV–visible spectrophotometer. Further more, the electrical properties have also been studied on the nanocrystalline films.

2. Experimental detail

Zinc selenide thin films were deposited onto cleaned, spectroscopic grade glass substrates. All chemicals used were of AR Grade. To synthesize nanocrystalline ZnSe, we have employed the chemical bath deposition (CBD) technique using zinc acetate and sodium selenosulphate as precursors of Zn²⁺ and Se²⁻ ions in the reaction system. To prepare sodium selenosulphate solution, 15g of sodium sulfite in 200ml water was refluxed with 5g of selenium for almost 10 hours at 80°C. The mixture remained under constant stirring throughout the reflux process. Selenosulphate is produced according to the following reaction:



Unreacted selenium is filtered off and selenosulphate solution is placed in air tight bottle. It is recommended to make small volumes of selenosulphate stock solution to be used within 3-4 days.

To deposit ZnSe, the solution is obtained by mixing an appropriate amount of 1 M zinc acetate with 2 M NaOH and with 80% hydrazine hydrate in a beaker. To this mixture, 20 ml of 1 M sodium selenosulphate is added slowly with constant stirring. The solution is stirred for few seconds and then transferred to another beaker containing substrates. Then the reactant vessel is kept in a constant temperature water bath maintained at 45°C which provides the external heat energy for ZnSe formation. The film formation does not take place at room temperature. This is because, at low temperatures, most of Zn²⁺ ions are in a bound state due to strong Zn–amine complex formation [14]. The deposition time is almost 3hrs. In the present paper the pH(11.0,12.0 and 13.0) is varied to study the effect of pH on properties of ZnSe thin film. The other parameters are kept constant. After deposition, the films are thoroughly washed with double distilled water and dried in air. The ZnSe nanocrystalline films obtained are uniform, well adherent to the substrates and white in colour.

The XRD patterns were collected with Rigaku Geigerflex equipment using nickel filtered CuK α radiation ($\lambda=1.54 \text{ \AA}$) in the 2θ range of 20°C to 80°C. The absorption spectra were recorded using double beam spectrophotometer [SPECORD-250] in the transmission range 200-800 nm for both samples. The electrical measurements of these thin films are carried out in a specially designed metallic sample holder where heat filtered white light of intensity 8450 lx (200W tungsten lamp) is shone through a transparent glass window. A vacuum of about 10 mbar was maintained throughout these measurements. Light intensity was measured using a digital luxmeter. Planar geometry of the films (length ~0.74 cm; electrode gap ~ 1mm) is used for the electrical measurements. Al electrodes are used for the electrical contacts because Al metal does not diffuse inside the material. These contacts are made by diffusion technique. The dark and photocurrent was noted using a digital picoammeter.

3. Result and discussion

3.1 Structural study

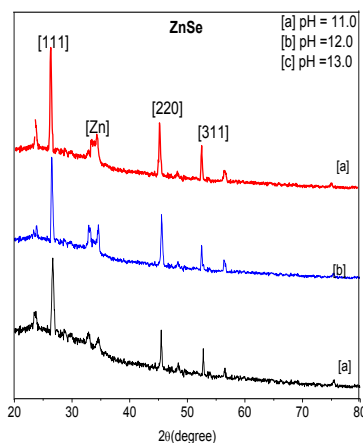


Fig. 1. XRD pattern of ZnSe thin films deposited at [a] pH=11.0 [b] pH=12.0 and [c] pH=13.0

The crystal size and structural phase of ZnSe nanocrystals have been obtained using X-ray diffraction spectra. ZnSe is known to exist in the hexagonal (wurtzite) as well as sphalerite (zinc blende) cubic phase or sometimes with a mixture of both the phases [15]. However, the wurtzite phase is obtained at high temperatures. As the hexagonal structure is a low energy structure, compared to cubic, it is supposed that the high surface energy of ZnSe nanocrystals compel it to retain cubic structure in the small size regime. Fig.1 shows the XRD pattern of ZnSe thin films deposited at three different pH(11.0,12.0 and 13.0). There is a highest intensity reflection peak at $2\theta = 26.29^\circ$ [1 1 1], with two another small intensity peaks at $2\theta = 45.29^\circ$ [2 2 0] and 52.88° [3 1 1]. Some new peaks of low intensity are also observed. The diffusion background and broad peaks are due to the amorphous glass substrate. The comparison of observed 'd' values with standard 'd' values [16] confirms that sphalerite (zinc blende) nanocrystalline structure of ZnSe thin films.

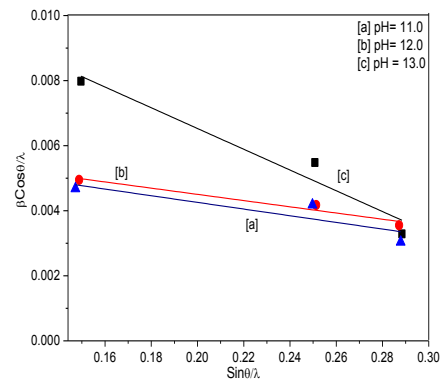


Fig. 2. Plots of $(\beta\cos\theta)/\lambda$ vs $(\sin\theta)/\lambda$ for ZnSe thin films at [a] pH= 11.0 [b] pH=12.0 and [c] pH = 13.0

Information of the strain and the particle size are obtained from the full width at half maximum (FWHMs) of the diffraction peaks. The FWHMs (β) can be expressed as a linear combination of the contributions from the strain (ϵ) and particle size (L) through the following relation [17]

$$\frac{\beta\cos\theta}{\lambda} + \frac{1}{L} = \frac{\epsilon\sin\theta}{\lambda} \quad (2)$$

Fig. 2 represents the plots of $(\beta\cos\theta)/\lambda$ vs. $(\sin\theta)/\lambda$ for ZnSe thin films at three different pH, which are straight lines. The slopes of these plots give the amount of residual strain. The reciprocal in intercepts on the $(\beta\cos\theta)/\lambda$ axis give the average particle size.

The value of particle size and strain are given in Table 1. The particle size increases as pH of the bath increases. At higher pH (in alkaline solution), generally selenosulphate decomposition is faster. It results in faster rate of reaction and hence particle size increases. The residual strain for these films deposited at different pH are negative which indicates the compressive strain. If the film deposited is free from impurities, the compressive strain is generated at the thin film substrate interface, when the very small crystallites are bonded to substrate, due to surface tension.

Table 1. Representation of the strain, particle size and optical band gap (E_g), ZnSe films deposited at different pH.

pH	Particle size(nm)	Strain	E_g (eV)
11.0	7.40	-0.0319	3.0
12.0	15.60	-0.0095	2.91
13.0	15.84	-0.0102	2.87

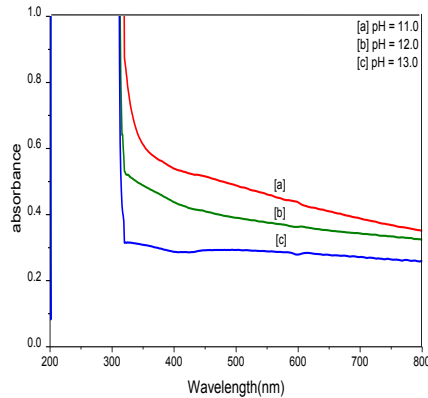


Fig. 3. Absorbance spectra of ZnSe thin films at [a] pH= 11.0 [b] pH=12.0 and [c] pH = 13.0

3.2 Optical study

Fig. 3 represents the absorption spectra of ZnSe thin films at different pH. From the absorption data, nearly at the fundamental absorption edge, the values of absorption coefficient (α), are calculated in the region of strong absorption using the relation:

$$\alpha = 2.303 \frac{A}{d} \quad (3)$$

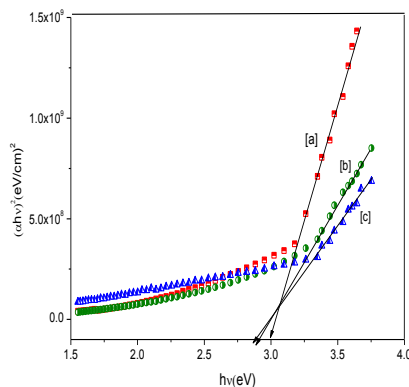


Fig. 4. The plots of $(ahv)^2$ vs. hv for ZnSe thin films at [a] pH= 11.0 [b] pH=12.0 and [c] pH = 13.0.

The fundamental absorption, which corresponds to the transition from valence band to conduction band, can be used to determine the band gap of the material. The relation between α and the incident photon energy ($h\nu$) can be written as [18]:

$$\alpha = \frac{A(h\nu - E_g)^n}{h\nu} \quad (4)$$

where A is a constant, E_g is the band gap of the material and the exponent n depends on the type of transition. The n may have values $1/2$, 2 , $3/2$ and 3 corresponding to the allowed direct, allowed indirect, forbidden direct and forbidden indirect transitions, respectively. The value of band gap E_g is calculated by extrapolating the straight line portion of $(\alpha h\nu)^{1/n}$ vs. $h\nu$ graph to $h\nu$ axis taking $n = 1/2$ (0.5). Fig. 4 show the plots of $(\alpha h\nu)^2$ vs. $h\nu$ for ZnSe films deposited at three different pH. The value of E_g at different pH is inserted in Table 1. E_g is found to decrease with the increase in pH as shown in Fig. 4. This is because, with increase in pH, particle size increases, as explained above. Clearly, the observed values of E_g are higher than the value of bulk optical gap of ZnSe (2.58 eV) due to quantum confinement in the ZnSe nanocrystallites.

3.3 Electrical properties

3.3.1 Steady state photoconductivity

Fig. 5 and Fig. 6 shows the temperature dependence of dark conductivity (σ_d) and photo conductivity (σ_{ph}) for thin films at different pH. The electrical conductivity shows typical Arrhenius type of activation

$$\sigma_d = \sigma_0 \exp\left(-\frac{\Delta\varepsilon}{kT}\right) \quad (5)$$

Where $\Delta\varepsilon$ is the activation energy for conduction and k is the Boltzmann's constant. Fig. 5 and Fig. 6 shows the variation of σ_d and σ_{ph} against $1000/T$ for ZnSe thin films deposited at different pH. The values of σ_d at room temperature increases as the pH of ZnSe thin films increases from 11.0 to 13.0 and the values of σ_{ph} at room temperature first decreases than increases as the pH of ZnSe thin films increases from 11.0 to 13.0. The increase in conductivity with the increase in pH Zn^{2+} ion is due to the increase in particle size of ZnSe NCs. The effect of size on electrical conductivity of nanostructures is based on the following mechanisms: surface scattering, quantized conduction, Coulomb charging and tunneling, widening and discrete band gap and change of micro structure. So, increase in conductivity of ZnSe thin films may be due to the decrease in grain boundary scattering, structural defects and dislocations and improvement of the nanoparticle size.

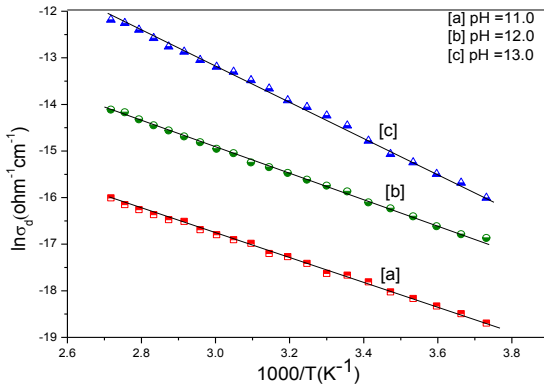


Fig. 5. Plot of (i) $\log \sigma_d$ vs. $(1000/T)$ of ZnSe films deposited at [a] pH = 11.0 [b] pH = 12.0 and [c] pH = 13.0.

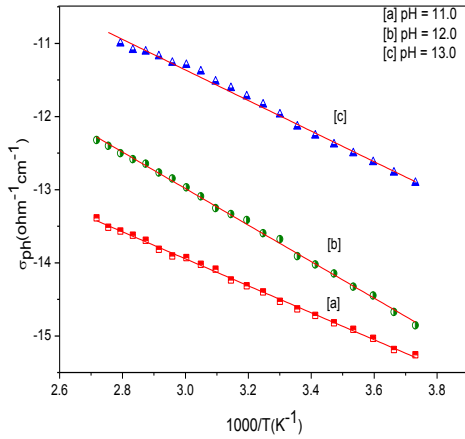


Fig. 6. Plot of $\log \sigma_{ph}$ vs. $(1000/T)$ of ZnSe films deposited at [a] pH = 11.0 [b] pH = 12.0 and [c] pH = 13.0.

It has been observed in Table 2 that there is increase in the value of activation energy ($\Delta \epsilon$) with the increase in pH. The similar type of results has been reported by some workers [19].

3.3.2 Transient photoconductivity

Fig. 7 shows the rise and decay curves of I_{ph} for ZnSe thin films at different pH. I_{ph} rises to a steady state value and decay of I_{ph} is slow. During decay, the photocurrent

does not reach zero for a long time after the incident light is switched off. A persistent photocurrent is observed in all the cases. This type of photoconductive decay has also been reported in various other semiconductors [20-22]. In the present case, the non-exponential decay of photoconductivity is observed.

The values of τ_d at different times have been calculated using equation

$$\tau_d = - \left[\frac{1}{I_{ph}} \frac{dI_{ph}}{dt} \right]^{-1} \quad (6)$$

For ZnSe thin films deposited at different pH of the solution from the slopes (at different times) of decay curves of Fig. 7.

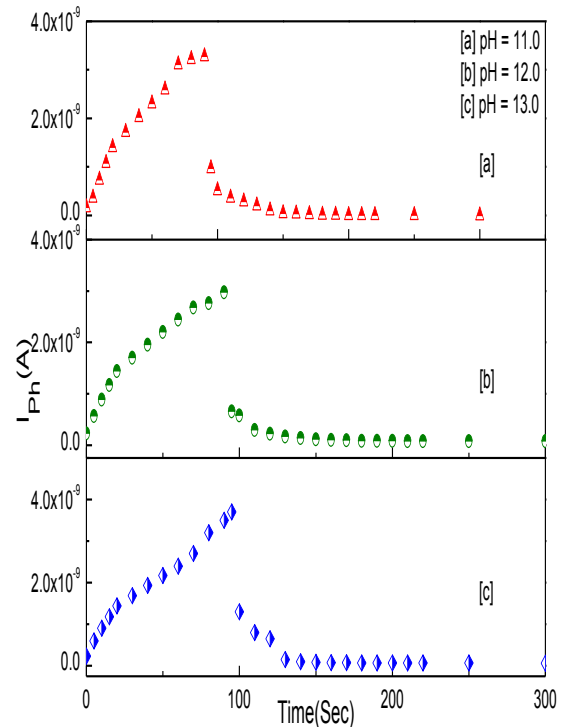


Fig. 7. The rise and decay curves of I_{ph} for ZnSe thin films at [a] pH = 11.0, [b] pH = 12.0 and [c] pH = 13.0.

Table 2. Variation of various electrical parameters for ZnSe thin films deposited at different pH values of the solution

pH	σ_d ($\Omega^{-1} \text{cm}^{-1}$)	E_d (eV)	σ_{ph} ($\Omega^{-1} \text{cm}^{-1}$)	E_{ph} (eV)	σ_{ph}/σ_d	$\ln \tau_d(t=0)$ (sec)
11.0	2.84×10^{-7}	0.51	1.92×10^{-6}	0.36	6.78	1.71
12.0	2.96×10^{-7}	0.55	1.68×10^{-6}	0.49	5.67	2.05
13.0	1.76×10^{-6}	0.75	8.67×10^{-6}	0.41	4.92	2.16

Fig. 8 shows the plots of $\ln \tau_d$ vs. $\ln t$ for all samples at intensity 8450 Lux. The extrapolation of the curves at $t = 0$, give the values of the carrier life time [17] and are

found to be 1.71, 2.05 and 2.16 seconds for films deposited at pH of the solution 11.0, 12.0 and 13.0. Clearly, the carrier life time increases with increasing pH

of the solution (size). The straight lines in Fig. 7, obey a power law of the form t^{-N} , with $N = d(\ln\tau_d/\ln t)$ and the values of N are found to be 0.305, 0.357 and 0.362 at pH of the solution 11.0, 12.0 and 13.0 respectively.

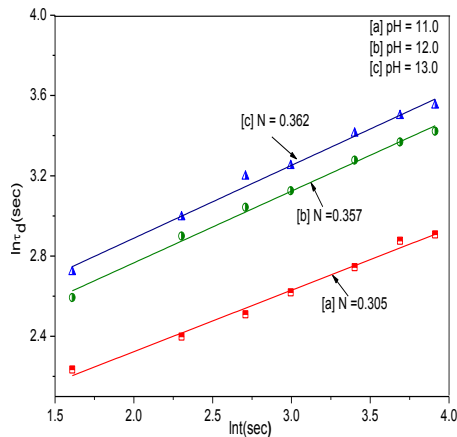


Fig. 8. Plot of τ_d vs. $\ln t$ for ZnSe thin films deposited at different pH [a] 11.0, [b] 12.0 and [c] 13.0.

4. Conclusions

Nanoparticles and thin films of ZnSe have been prepared using CBD technique at three different pH. The effect of pH on structural, optical and electrical properties has been studied. The size of the nanoparticles has been found of the order of 7-16nm which increases with increase of pH and structure of the nanoparticles obtained is zinc-blende. The band gap decreases from 3.0 eV to 2.87 eV with the increase in pH of the bath. Electrical parameters like dark and photoconductivity increase as the particle size increases and activation energy also increases with increase in pH. In the rise and decay curves of pH, the non-exponential decay of photoconductivity is observed and the photocurrent does not reach zero for a long time after the incident light is switched off. The carrier life time τ_d increases with increase of pH of the solution.

Acknowledgements

The author acknowledges the support provided by Mr. S.C. Sood of Ambala College of Engineering, Mithapur for the completion of this work.

References

- [1] A. Gaur, D. K. Sharma, D. S. Ahlawat, N. Singh, J. Opt. A, Pure Appl. Opt. **9**(3), 260 (2007).
- [2] B. Ludolph, M. A. Malik, P. O. Brien, N. Revaprasadu, Chem. Commun. **17**, 1849 (1998).
- [3] J. Yang, C. Xue, S. H. Yu, J. H. Zeng, Y. T. Qian, Angew.Chem., **114**(24), 4891(2002).
- [4] Q. Peng, Y. J. Dong, Y. D. Li, Angew. Chem. Int. Edn **42**, 3027 (2003).
- [5] T. L. Chu, S. S. Chu, Prog. Photovoltaics Res. Appl. **1**(1), 31 (1993).
- [6] A. Fedorov, K. Katrunov, A. Lalayants, V. Nesterkina, N. Shiran, S. Tretyak, IEEE Trans. Nucl. Sci. **55**(3), 1561 (2008).
- [7] T. Zhang, Y. Shen, W. Hu, J. Sun, J. Wu, Z. Ying, N. Xua, J. Vac. Sci. Technol. **B25**, 1823 (2007).
- [8] A. Colli, S. Hofmann, A. C. Ferrari, F. Martelli, S. Rubini, C. Ducati, A. Franciosi, J. Robertson, Nanotechnol. **16**, S139 (2005).
- [9] R. Henriquez, H. Gomez, G. Riveroz, J. F. Gullimoles, M. Froment, D. Lincot, J. Phys. Chem. B, **108**, 13191 (2004).
- [10] Bedir, M. Oztas, O. F. Bakkaloglu, R. Ormanci, Euro. Phys. J. **B45**, 465 (2005).
- [11] H. Q. Jiang, J. Che, X. Yao, T. Nonferr. Met. Soc. **16**, 266 (2006).
- [12] X. T. Zhang, K. M. Ip, Z. Liu, Y. P. Leung, Q. Li, S. K. Hark, Appl. Phys. Lett. **84**, 2641 (2004).
- [13] C. Mehta, G.S.S. Saini, Jasim M. Abbas, S. K. Tripathi, Applied Surface Science **256**, 608 (2009).
- [14] G. Hodes, Marcel Dekker, New York, Basel, 2003.
- [15] R. B. Kale, C. D. Lokhande, Appl. Surf. Sci. **225**, 929 (2005).
- [16] JCPDS data files 37-1463 and 15-105.
- [17] S. B. Quadri, E. F. Skelton, D. Hsu, A. D. Dinsmore, J. Yang, H. F. Gray, B. R. Ratna, Phys.Rev. **B60**, 9191 (1999).
- [18] J. J. Pankove, Prentice-Hall, Englewood Cliffs, NJ, 1971.
- [19] G. I. Rusu, M. E. Popa, G. G. Rusu, I. Salaoru, Appl. Surf. Sci. **218**, 222(2005).
- [20] V. Sharma, A. Thakur, P.S. Chandel, N. Goyal, G. S. S. Saini, S. K. Tripathi, J. Optoelectron. Adv. M. **5**, 1243 (2003).
- [21] D. V. Harea, I. A. Vasilev, E. P. Colomeico, M. S. Iovu, J. Optoelectron. Adv. M. **5**, 1115 (2003).
- [22] M. S. Iovu, S. D. Shutov, V. I. Arkhipov, G. J. Adriaenssens, J. Non-Cryst.Solids **299**, 1008 (2002).

*Corresponding author: deep_shikha79@yahoo.co.in